Letter

An amphiphilic micromolecule self-assembles into vesicles for visualized and targeted drug delivery

Weiwei Ma, Jingjing Bi, Hao Wu, and Guisheng Zhang

ACS Med. Chem. Lett., **Just Accepted Manuscript** • DOI: 10.1021/acsmedchemlett.0c00212 • Publication Date (Web): 20 Jul 2020

An amphiphilic micromolecule self-assembles into vesicles for visualized and targeted drug delivery

Weiwei Ma,[a,b] Jingjing Bi,*[a] Hao Wu,[a] Guisheng Zhang*[a]

[a] Key Laboratory of Green Chemical Media and Reactions, Ministry of Education, Collaborative Innovation Center of Henan Province for Green Manufacturing of Fine Chemicals, Henan Key Laboratory of Organic Functional Molecule and Drug Innovation, School of Chemistry and Chemical Engineering, Henan Normal University, Xinxiang, Henan 453007, China.

[b] College of Pharmacy, Xinxiang Medical University, China.

*Fax: (+86)-373-332-5250; E-mail: zgs@htu.cn or bijingjing2008@126.com

ABSTRACT: Described here is the first example for constructing multifunctional drug delivery systems by employing an amphiphilic micromolecule. The intrinsic aggregation-induced emissive and tumor-targeting amphiphilic conjugate of β-D-galactose with tetraphenylethene (TPE-Gal), in which the hydrophobic TPE moiety spontaneously acts as the imaging chromophore and hydrophilic Gal moiety spontaneously as the targeting ligand and galactosidase trigger, can self-assemble into fluorescent vesicles that can efficiently load both water-soluble and -insoluble anticancer drugs. In vitro and in vivo evaluations revealed that the pH/β-D-galactosidase dual responsive doxorubicin-loaded vesicles TPE-Gal@DOX exhibited good targeting effect and higher anti-tumor efficacy than free doxorubicin. H&E staining analysis displayed remarkable necroses and weak cell proliferation in the tumor area, and no toxicity to major organs, indicating the superior targeting anti-tumor therapeutic efficacy of TPE-Gal@DOX.

KEYWORDS. β-D-galactose-modified tetraphenylethenes, aggregation-induced emission, fluorescent vesicles, cell imagimg, targeted drug delivery.

Chemotherapy is an indispensable cancer-treatment method. However, the poor pharmacokinetics and lack of tumor-targeting of the conventional chemotherapeutic drugs limited their clinic uses.[1-3] Drug delivery systems (DDSs) are essential for improving the effectiveness of chemotherapy.[4-8] Over the past years, amphiphilic block copolymers self-assembled into liposomes, micelles, or vesicles in selective solvents as DDSs in the use of cancer-treatment have attracted much attention.[9-11] Recent researches concerning DDSs stressed on multi-functionalization that can achieve targeted delivery and triggered the release of the drugs inside targeted cells, as well as the real-time monitoring of drug localization.[12-16] The general multi-functionalization method was to physically wrap or chemically integrate a fluorescent dye and a targeting unit into the self-assembled skeletons to construct a visualized and targeted DDS. However, with such functionalizations, the physical and chemical properties of DDSs may be changed; the behavior of labelled DDSs in endocytosis or phagocytosis may be different from that of unlabeled DDSs; fluorescent dyes may be hydrolyzed and dissociated from DDS during phagocytosis;[17] Especially, the toxicity and aggregation caused quenching (ACQ) characteristics of traditional fluorescent dyes seriously limit their applications.[18] Since the first reported aggregation-induced emission (AIE) phenomenon by Tang *et al*.,[19] fluorescent nano-particles based on AIE active tetraphenylethene (TPE) chromophores[20] have emerged in bioimaging and drug delivery.[21-26] These TPE-based copolymers or coordination polymer nanoparticles used for target drug delivery can efficiently address ACQ drawbacks of traditional fluorescent-labelled multi-functional DDS.

It is noteworthy that almost all of the known nanoparticle DDSs of liposomes, micelles, and vesicles were constructed by the self-assemblies of amphiphilic polymers. However, the polymeric DDSs have some manufacturing-related problems like low drug entrapment and stability problems due to the sensitive degradation of the polymer main chain or the spontaneous escape of the nanoparticles.[27-28] Therefore, if multi-functional DDSs were self-assembled by amphiphilic micromolecules with intrinsic AIE and targeting characteristics (instead of wrapping or integrating a fluorescent dye and a targeting unit into polymeric skeletons), it would be a new generation of multi-functional DDSs overcoming most of the drawbacks of the traditional multi-functional DDSs. Herein, we present an intrinsic AIE and tumor-targeting amphiphilic micromolecule, a conjugate of tetraphenylethene with β-D-galactose (TPE-Gal), which can facilely self-assemble into the pH/β-D-galactosidase dual responsive vesicles for cancer cell imaging, targeted drug delivery and chemotherapy (Scheme 1). The hydrophobic TPE moiety of the novel amphiphile spontaneously acts as the imaging chromophore, and Gal moiety spontaneously as the targeting ligand and galactosidase trigger.

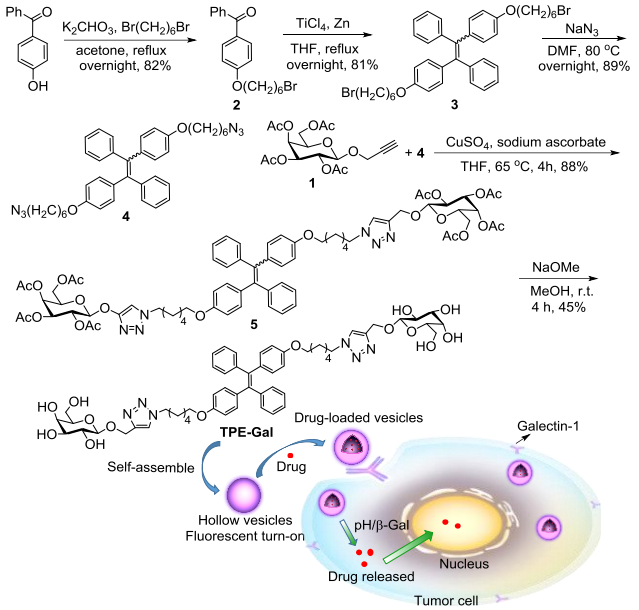

Scheme 1. The synthesis of TPE-Gal and TPE-Gal vesicles generating for visualized and targeted drug delivery.

Galectin-1, a 14-kD laminin-binding lectin that widely expressed in and around the membrane of various solid tumors cells,[29-30] can bind to β-galactosides through a rigorous carbohydrate recognition domain.[31] Meanwhile, β-galactosidase, a lysosomal enzyme that is known to be upregulated in various cancer subtypes, can be utilized to activate galactoside-containing DDSs.[32-36] Based on the AIE behavior of hydrophobic TPE and the unique tumor-targeting ability of hydrophilic β-galactose, a rational design for developing novel visualized and target anticancer DDSs has emerged: The conjugates of TPE with β-D-galactose self-assemble into uniform and robust vesicles to load anticancer drugs. To be our best knowledge that employing amphiphilic micromolecules in construction of DDSs has not been reported.

The synthesis of TPE-Gal was illustrated in Scheme 1. The reaction of 4-hydroxybenzophenone with 1,6-dibromohexane in the presence of K_2CO_3 afforded **2**, from which the TPE derivatives **3** were obtained through the McMurry reaction.[37] Further treatment of **3** with excess NaN_3 gave azido compounds **4**. Finally, TPE-Gal was synthesized using classic CuAAC reaction between **4** and propargyl 2,3,4,6-tetra-*O*-acetyl-β-D-galactoside **1** followed by the global deacetylation with NaOMe/MeOH.

TPE-Gal exhibited extremely weak fluorescence in DMSO (10 μM) and the maximum peaks generally located at 390 nm. However, with the addition of water, the fluorescence intensity dramatically increased, and the maximum emission was broadened and red-shifted to 473 nm (Figure. S1). When the water fraction reached to 90%, the fluorescence intensity of TPE-Gal was nearly 50-fold stronger than in pure DMSO, indicating the AIE characteristics of TPE-Gal. The morphology of TPE-Gal vesicles was observed by TEM (Figure 1A) and exhibited a hollow spherical shape with the particle-size of about 120 nm. In addition, the dynamic light scattering (DLS) assay (Figure S2) demonstrated that the average hydrodynamic size and the polydispersity index of TPE-Gal vesicles are 157.4 ± 7.69 nm and 0.074 respectively, disclosing that the vesicles have a relatively homogenous size and well dispersibility in aqueous media without significant aggregation. The difference in particle-size between TEM and DLS can be attributed to the technique of measurement conditions. The zeta potential (Figure S3) of TPE-Gal vesicles was determined to be -25 ± 2.3 mV. It has been well known that 150 nm nanoparticles with slightly negative charge have the good stability under the physiological conditions and tend to accumulate in tumor more efficiently.[38] The TPE-Gal vesicles was stable in water， PBS and plasma of mice over multiple weeks without significant aggregation (Figure S4).

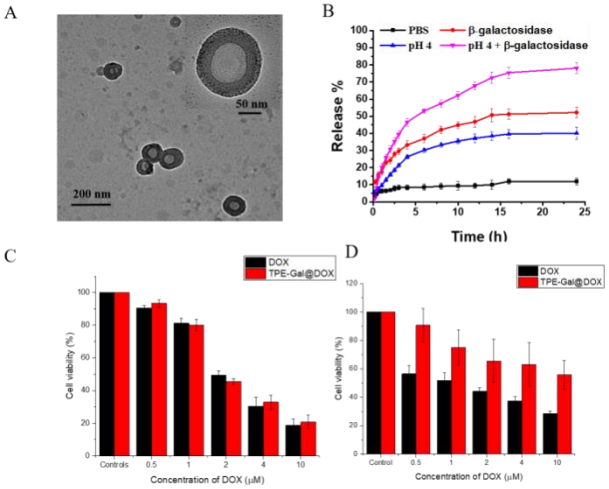

Figure 1. TEM photograph of TPE-Gal vesicles (A); Cumulated release profiles of DOX from TPE-Gal@DOX in different media (B); Cell viabilities of TPE-Gal@DOX and free DOX to HepG2 cells (C) and normal L02 cells (D).

Water-soluble doxorubicin (DOX) and water-insoluble paclitaxel (PTX) were chosen as model drugs to investigate the loading capacity of TPE-Gal vesicles. TPE-Gal vesicles show a decent DOX loading capacity with drug-loading contents (DLC) of 15.4 wt%, which corresponded to encapsulation efficiency (EE) of 88.5%. Furthermore, TEM images (Figure S5) have clearly shown the morphology of the DOX-loaded vesicles TPE-Gal@DOX was spherical and had good dispersion with a diameter of 165.2 ± 8.31 nm (Figure S6) and zeta potential of -17.1 ± 4.4 mV (Figure S7). Similarly, TPE-Gal@PTX also showed good PTX loading capacity with DLC of 7.6 wt% and EE of 82.3%.

UV-Vis absorption (Figure S8), IR spectra (Figure S9) and fluorescence spectra (Figure S10) of different samples demonstrated the successful fabrication of the TPE-Gal@DOX. Moreover, the distribution state of DOX in TPE-Gal@DOX was detected by DSC methods (Figure S11). The DSC thermogram of DOX shows one endothermic peak at 218 °C, while it cannot be observed for TPE-Gal@DOX, indicating that DOX disperses in vesicles with an amorphous state instead of crystalline state. This result has also strongly proved the successful fabrication of the TPE-Gal@DOX.

For an ideal DDS, it is critical to release the drug triggered by the stimuli associated with the specific microenvironmental changes. Under intracellular-mimicking high expression of galactosidase conditions (in the presence of 100U β-galactosidase), DOX can be rapidly released from TPE-Gal@DOX (Figure 1B), in which the cumulative DOX releases are ca. 25% and 50% in 2 h and 12 h, respectively. In contrast, less than 10% drug release is observed in 12 h for TPE-Gal@DOX in the absence of galactosidase. Moreover, the fluorescence change

could be detected with the naked eye under UV light (365 nm; Figure S12). It's well known that the microenvironment of tumor tissues is more acidic than normal tissues. Then, the controllable DOX release under different pH was carried out. As shown in Figure 1B, the release of DOX from TPE-Gal@DOX was pH- and time-dependent. Consequently, the pH/β-galactosidase dual-responsive release behavior of TPE-Gal@DOX provides a theoretical basis for safe and efficient tumor chemotherapy.

The determination of hemolytic properties is a common biocompatibility test in drug carrier development. After 4 h of incubation, there was no obvious hemolysis under different concentrations of TPE-Gal, even at high dosage (Figure S13, S14). It caused only 4.78 ± 1.04% hemolysis in fresh human blood at 1000 μg/mL concentration, suggesting that TPE-Gals possess high hemocompatibility and low toxicity. The MTT assay showed that the cytotoxicity of TPE-Gal vesicles to HepG2 cells was similar to controls (Figure S15), the cells retained 85% viability even at a maximum concentration of 100 μg/mL. TPE-Gal@DOX and free DOX had almost the same anti-proliferative effects on ~~of~~ cancer cells at the same concentration of DOX (Figure 1C). Moreover, compared to free DOX, the TPE-Gal@DOX showed ~~a~~ significantly low cytotoxicity to normal L02 cells (Figure 1D). These results indicated that the vesicles formulation had the capability of delivering DOX molecules into tumor cells, causing the intracellular release and leading to cytotoxicity.

The cellular uptake of TPE-Gal@DOX was evaluated by confocal laser scanning microscopy (CLSM). As shown in Figure 2A, in CLSM images using the blue (TPE) and red (DOX) fluorescent channels, the fluorescence intensity steadily increased over time, suggesting the efficient uptakes of vesicles by HepG2 cells and the successful drug release from the TPE-Gal@DOX in a time-dependent manner. After treated with TPE-Gal@DOX for 0.5 h, HepG2 cells exhibited distinct fluorescence, each cell showed a region of particularly high fluorescence intensity where both TPE and DOX were gathered. We hypothesized that this region might correspond to lysosomes, where the releasing of DOX from the TPE-Gal@DOX led to the fluorescence of both TPE and DOX. "After two hours of incubation, the fluorescence of TPE only appeared in lysosomes, but not in the nucleus, indicating that the vesicles just performs its delivery function and does not influence the biological fate of the drug. In the DOX fluorescence channel, the DOXs were released from vesicles in the lysosome and translocated into the cell nucleus. However, compared to HepG2 cells, similar TEP fluorescence but weak DOX fluorescence has been observed at the same time for L02 cells. These phenomena illustrated that the TPE-Gal vesicles can be taken efficiently by cells for imaging, but only exhibit a sustained drug-releasing pattern in tumor cells. Furthermore, the blue fluorescence of TPE from TPE-Gal vesicles mostly colocalized with the "green" fluorescence of lysotracker near the nucleus (Figure 2B), indicating the indeed colocalization of TPE-Gal with lysosomes.

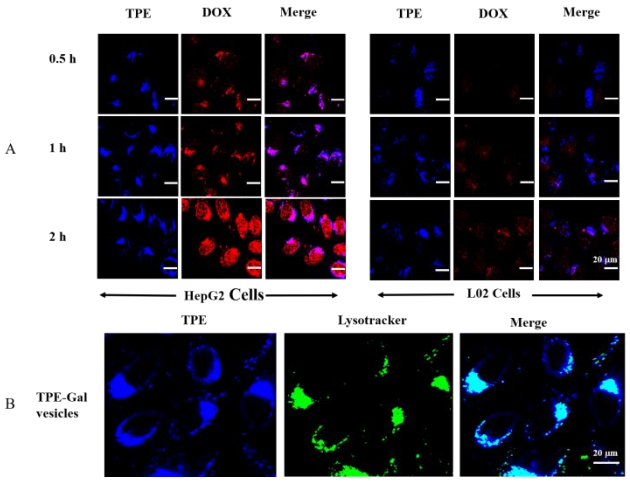

Figure 2. CLSM images of the cellular uptake and controlled release behaviors of HepG2 cells and L02 cells (A); CLSM images of HepG2 cells in TPE-Gal vesicles (B).

Encouraged by the exciting results *in vitro* evaluations, the *in vivo* antitumor efficacy and tumor-targeting effect of TPE-Gal@DOX were evaluated in tumor-bearing mice by giving drugs intravenously. As shown in Figure 3A, the average tumor volume in the mice treated with saline solely and the blank TPE-Gal vesicles increased rapidly. In strong comparison, the tumor volume in the animals treated with free DOX increased slowly. To our delight, TPE-Gal@DOX exhibited ~~obviously~~ stronger inhibition effect on tumor growth compared with the free DOX group (Figure S16), which might attribute to the enhanced cellular uptake of TPE-Gal@DOX by targeted delivery and pH/β-galactosidase-sensitive drug release at tumor sites. The biodistribution of DOX clearly expressed the amount of drug in each tissue (Figure S17). According to the results, distribution of TPE-Gal@DOX was significantly lower in heart, spleen, lung and kidney compared to that of free DOX, implying that DOX can be gradually eliminated in major organs with the time extending. Notably, TPE-Gal@DOX achieved the highest concentration in the tumor by comparison to free DOX. Photographs of tumors on day 21 after the treatment also showed that TPE-Gal@DOX inhibited the tumor growth much better than free DOX (Figure 3C). In addition, as shown in Figure 3B, TPE-Gal@DOX showed no obvious influence on the bodyweight of mice, implying good biocompatibility of this delivery system. The histological examination of the tumors and main organs were evaluated after 21 days of treatment. As shown in Figure 3D, the H&E staining of sectioned tumor tissues showed that increased apoptosis of tumor cells was observed in the groups of TPE-Gal@DOX compared with tissues in other groups, further indicating the superior antitumor therapeutic efficacy of TPE-Gal@DOX. Furthermore, the TPE-Gal@DOX groups showed no apparent morphological difference among the saline groups in heart, liver, spleen, lung, or kidney, proving that TPE-Gal@DOX caused no harm to the mice (Figure S18). All of the results implied that TPE-Gal vesicle is a very promising tumor-targeting drug carrier for cancer chemotherapy.

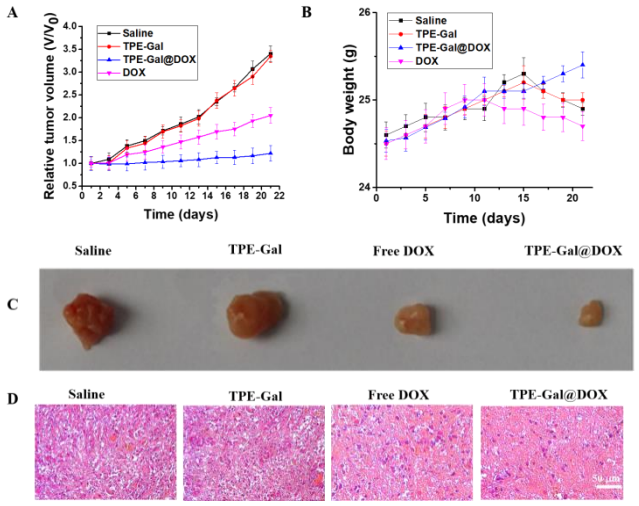

Figure 3. Growth curves of the relative tumor volume (A); Bodyweight of tumor-bearing mice (B); Photographs of tumors excised on day 21 after treatment (C); H&E staining of tumor (D).

In summary, a brand-new strategy for constructing multifunctional DDSs through self-assembly of intrinsic AIE and tumor-targeting amphiphilic micromolecules has been developed to overcome the drawbacks of traditional DDSs functionalized by wrapping or integrating a fluorescent dye or a targeting unit into polymeric carrier skeletons. The synthesized amphiphile TPE-Gal can facilely self-assemble into uniform and robust vesicles with the average hydrodynamic sizes of 157.4 ± 7.69 nm and the zeta potential of -25 ± 2.3 mV, disclosing that the vesicles could efficiently tend to accumulate in tumors. In vitro and in vivo investigations demonstrated that such nano-vesicles with high biocompatibility can efficiently load both water-soluble and water-insoluble anticancer drugs, and the drug-loaded vesicles showed a remarkably selective toxicity to tumor cells and a significantly higher anti-tumor efficacy than free drugs. Therefore, the first generation of pH/β-galactosidase dual responsive TPE-Gal vesicles DDSs are suitable for the visualized and targeted anticancer drug delivery and the treatment of solid tumors. This work might provide a new perspective of developing new generation of multifunctional DDSs.

ASSOCIATED CONTENT

Supporting Information

The Supporting Information is available free of charge on the ACS Publications website.

Additional figures as described in the text; synthetic and activity test procedures, and spectral data of the target compounds (PDF)

AUTHOR INFORMATION

Corresponding Author

* Guisheng Zhang: E-mail: zgs@htu.cn; orcid.org/ 0000-0001-9880-950X

Jingjing Bi: E-mail: bijingjing2008@126.com; orcid.org/0000-0002-3842-0954

Author Contributions

All authors have given approval to the final version of the manuscript.

Funding Sources

Notes

The authors declare no competing financial interest.

ACKNOWLEDGMENT

We thank the NSFC (U1604285 and 21877206), PCSIRT (IRT1061), the 111 Project (D17007).

ABBREVIATIONS

TPE, tetraphenylethene; Gal, β-D-galactose; DOX, doxorubicin; PTX, paclitaxel; DDS, drug delivery system; ACQ, aggregation caused quenching; AIE, aggregation-induced emission; DMSO, dimethyl sulfoxide; DLS, dynamic light scattering; TEM, transmission electron microscope; DLC, drug-loading contents; EE, encapsulation efficiency; DSC, differential scanning calorimetry; UV-Vis, ultraviolet and visible spectrophotometry; IR, infrared radiation; CLSM, confocal laser scanning microscopy; H&E, hematoxylin and eosin.

REFERENCES

(1) Riehemann, K.; Schneider, S. W.; Luger, T. A.; Godin, B.; Ferrari, M.; Fuchs, H. Nanomedicine—challenge and perspectives. *Angew. Chem. Int. Ed.* **2009**, *48*, 872-897.

(2) Karthika, V.; Kaleeswarran, P.; Gopinath, K.; Arumugam, A.; Govindarajan, M.; Alharbi, N. S.; Khaled, J. M.; Al-Anbr, M. N.; Benelli, G. Biocompatible properties of nano-drug carriers using TiO2-Au embedded on multiwall carbon nanotubes for targeted drug delivery. *Mater. Sci. Eng. C Mater. Biol. Appl.* **2018**, *90*, 589-601.

(3) Guha, P.; Roy, B.; Nahak, P.; Karmakar, G.; Chang, C. H.; Bikov, A. G.; Akentiev, A. B.; Noskov, B. A.; Mandal, A. K.; Kumar, A.; Hassan, P. A.; Aswal, V. K.; Misono, T.; Torigoe, K.; Panda, A. K. Exploring the dual impact of hydrocarbon chainlength and the role of piroxicam a conventional NSAID on soylecithin/ion pair amphiphiles mediated hybrid vesicles for brain-tumor targeted drug delivery. *Colloids and Surfaces A: Physicochem. Eng. Aspects*. **2018**, *546*, 334-345.

(4) Tibbitt, M. W.; Dahlman, J. E.; Langer, R. Emerging frontiers in drug delivery. *J. Am. Chem. Soc*. **2016**, *138*, 704-717.

(5) Wilhelm, S.; Tavares, A. J.; Dai, Q.; Ohta, S.; Audet, J.; Dvorak, H. F.; Chan, W. C. Analysis of nanoparticle delivery to tumours. *Nat. Rev. Mater*. **2016**, *1*, 16014.

(6) Yu, J.; Chen, Y; Zhang, Y. H.; Xu, X.; Liu, Y. Supramolecular assembly of coronene derivatives for drug delivery. *Org. Lett.* **2016**, *18*, 4542-4545.

(7) Kostka, L.; Kotrchová, L.; Šubr, V.; Libánská, A.; Ferreira, C. A.; Malátová, I.; Lee, H. J.; Barnhart, T. E.; Engle, J. W.; Cai, W.; Šírová, M.; Etrych, T. HPMA-based star polymer biomaterials with tuneable structure and biodegradability tailored for advanced drug delivery to solid tumours. *Biomaterials*. **2020**, *235*, 119728.

(8) Xia, D.; Li, Y.; Jie, K.; Shi, B.; Yao, Y. A Water-soluble cyclotriveratrylene-based supra-amphiphile: synthesis, pH-responsive self-assembly in water, and its application in controlled drug release. *Org. Lett.* **2016**, *18*, 2910-2913.

(9) Wicki, A.; Witzigmann, D.; Balasubramanian, V.; Huwyler, J. Nanomedicine in cancer therapy: challenges, opportunities, and clinical applications. *J. Control. Release*. **2015**, *200*, 138-157.

(10) Discher, D. E.; Eisenberg, A. Polymer vesicles. *Science*, **2002**, *297*, 967-973;

(11) Maeda, H.; Nakamura, H.; Fang, J. The EPR effect for macromolecular drug delivery to solid tumors: improvement of tumor uptake, lowering of systemic toxicity, and distinct tumor imaging in vivo. *Adv. Drug Deliv. Rev.*, **2013**, *65*, 71-79.

(12) Rahimi, M.; Safa, K. D.; Alizadeh, E.; Salehi, R. Dendritic chitosan as a magnetic and biocompatible nanocarrier for the

simultaneous delivery of doxorubicin and methotrexate to MCF-7 cell line. *New J. Chem.* **2017**, *41*, 3177-3189.
(13) Prabaharan, M.; Grailer, J. J.; Pilla, S.; Steeber, D. A.; Gong, S. Gold nanoparticles with a monolayer of doxorubicin-conjugated amphiphilic block copolymer for tumor-targeted drug delivery. *Biomaterials*, **2009**, *30*, 6065-6075.
(14) Rejeeth, C.; Vivek, R.; NipunBabu, V.; Sharma, A.; Ding, X.; Qian, K. Cancer nanomedicine: from PDGF targeted drug delivery *Med. Chem. Comm.* **2017**, *8*, 2055-2059.
(15) Srinivasarao, M.; Galliford, C. V.; Low, P. S. Principles in the design of ligandtargeted cancer therapeutics and imaging agents. *Nat. Rev. Drug Discov*. **2015**, *14*, 203-219.
(16) Paul, A.; Biswas, A.; Sinha, S.; Shah, S. S.; Bera, M.; Mandal, M.; Singh, N. D. P. Push–pull stilbene: visible light activated photoremovable protecting group for alcohols and carboxylic acids with fluorescence reporting employed for drug delivery. *Org. Lett.* **2019**, *21*, 2968-2972.
(17) Xue, X.; Zhao, Y.; Dai, L.; Zhang, X.; Hao, X; Zhang, C.; Huo, S.; Liu, J.; Liu, C.; Kumar, A.; Chen, W. Q.; Zou, G.; Liang, X. J. Spatiotemporal drug release visualized through a drug delivery system with tunable aggregation-induced emission. *Adv. Mater*. **2014**, *26*, 712-717.
(18) Wang, X.; Yang, Y.; Yang, F.; Shen, H.; Wu, D. pH-triggered decomposition of polymeric fluorescent vesicles to induce growth of tetraphenylethylene nanoparticles for long-term live cell imaging. *Polymer*. **2017**, *118*, 75-84.
(19) Luo, J.; Xie, Z.; Lam, J. W. Y.; Cheng, L.; Tang, B. Z.; Chen, H.; Qiu, C.; Kwok, H. S.; Zhan, X.; Liu, Y.; Zhu, D.; Tang, B. Z. Aggregation-induced emission of 1-methyl-1,2,3,4,5-pentaphenylsilole. *Chem. Commun.* **2001**, *18*, 1740-1741.
(20) Tong, H.; Hong, Y.; Dong, Y.; Haussler, M.; Lam, J. W.; Li, Z.; Guo, Z.; Guo, Z.; Tang, B. Z. Fluorescent ''light-up'' bioprobes based on tetraphenylethylene derivatives with aggregation-induced emission characteristics. *Chem. Commun.* **2006**, *35*, 3705-3707.
(21) Han, X.; Liu, D. E.; Wang, T.; Lu, H.; Ma, J.; Chen, Q.; Gao, H. Aggregation-induced-emissive molecule incorporated into polymeric nanoparticulate as FRET donor for observing doxorubicin delivery. *ACS Appl. Mater. Interfaces.* **2015**, *7*, 23760-23766.
(22) Song, S.; Zheng, Y. S. Hollow spheres self-assembled by a tetraphenylethylene macrocycle and their transformation to bird nests under ultrasound. *Org. Lett.* **2013**, *15*, 820-823.
(23) Li, M.; Hong, Y.; Wang, Z.; Chen, S.; Gao, M.; Kwok, R. T.; Qin, W.; Lam, J. W.; Zheng, Q.; Tang, B. Z. Fabrication of chitosan nanoparticles with aggregation-induced emission characteristics and their applications in long-term live cell imaging. *Macromol. Rapid. Commun.* **2013**, *34*, 767-771.
(24) Yu, G.; Zhang, M.; Saha, M. L.; Mao, Z.; Chen, J.; Yao, Y.; Zhou, Z.; Liu, Y.; Gao, C.; Huang, F.; Chen, X.; Stang, P. J. Antitumor activity of a unique polymer that incorporates a fluorescent self-assembled metallacycle. *J. Am. Chem. Soc.* **2017**, *139*, 15940-15949.
(25) Wang, L.; Wang, W.; Xie, Z. Tetraphenylethylene-based fluorescent coordination polymers for drug delivery. *J. Mater. Chem. B.* **2016**, *4*, 4263-4266.
(26) Ye, F.; Liu, Y.; Chen, J.; Liu, S. H.; Zhao, W.; Yin, J. Tetraphenylene-coated near-infrared benzoselenodiazole dye: AIE behavior, mechanochromism, and bioimaging. *Org. Lett.* **2019**, *21*, 7213-7217.
(27) Wan, Q.; Liu, M.Y.; Xu, D. Z.; Huang, H. Y.; Mao, L. C.; Zeng, G. J.; Deng, F. J.; Zhang, X. Y.; Wei, Y. Facile fabrication of amphiphilic AIE active glucan via formation of dynamic bonds: self assembly, stimuli responsiveness and biological imaging. *J. Mater. Chem. B.* **2016**, *4*, 4033-4039.
(28) Wang, X.; Yang, Y. Y.; Zuo, Y .F.; Yang, F.; Shen, H.; Wu, D. C. Facile creation of FRET systems from a pH-responsive AIE fluorescent vesicle. *Chem. Commun.* **2016**, *52*, 5320-5323.
(29) Rabinovich, G. A. Galectin-1 as a potential cancer target. *Br. J. Cancer.* **2005**, *92*, 1188-1192.
(30) Liu, F. T.; Rabinovich, G. A. Galectins as modulators of tumour progression. *Nat. Rev. Cancer*. **2005**, *5*, 29-41.
(31) Thijssen, V. L.; Hulsmans, S.; Griffioen, A. W. The galectin profile of the endothelium altered expression and localization in activated and tumor endothelial cells. *Am. J. Pathol.* **2008**, *172*, 545-553.
(32) Asanuma, D.; Sakabe, M.; Kamiya, M.; Yamamoto, K.; Hiratake, J.; Ogawa, M.; Kosaka, N.; Choyke, P. L.; Nagano, T.; Kobayashi, H.; Urano, Y. Sensitive β-galactosidase-targeting fluorescence probe for visualizing small peritoneal metastatic tumours in vivo. *Nat. Commun.* **2015**, *6*, 6463.
(33) Sharma, A.; Kim, E. J.; Shi, H.; Lee, J. Y.; Chung, B. G.; Kim, J. S. Development of a theranostic prodrug for colon cancer therapy by combining ligand-targeted delivery and enzyme-stimulated activation. *Biomaterials.* **2018**, *155*, 145-151.
(34) Legigan, T.; Clarhaut, J.; Tranoy-Opalinski, I.; Monvoisin, A.; Renoux, B.; Thomas, M.; Le Pape, A.; Lerondel, S.; Papot, S. The first generation of *β*-galactosidase-responsive prodrugs designed for the selective treatment of solid tumors in prodrug monotherapy. *Angew. Chem. Int. Ed.* **2012**, *51*, 11606-11610.
(35) Liu, X.; Shao, W.; Zheng, Y.; Yao, C.; Peng, L.; Zhang, D.; Hu, X. Y.; Wang, L. GSH-responsive supramolecular nanoparticles constructed by *β*-D-galactose-modified pillar[5]arene and camptotecin prodrug for targeted anticancer drug delivery. *Chem. Commun.* **2017**, *53*, 8596-8599.
(36) Yang, K.; Yang, K.; Chao, S.; Wen, J.; Pei, Y.; Pei, Z. A supramolecular hybrid material constructed from pillar[6]arene-based host-guest complexation and ZIF-8 for targeted drug delivery. *Chem. Commun.* **2018**, *54*, 9817-9820.
(37) Dong, Y.; Wang, W.; Zhong, C.; Shi, J.; Tong, B.; Feng, X.; Zhi, J.; Dong, Y. Investigating the effects of side chain length on the AIE properties of water-soluble TPE derivatives. *Tetrahedron Lett.* **2014**, *55*, 1496-1500.
(38) Yu, Q.; Wei, Z.; Shi, J.; Guan, S.; Du, N.; Shen, T.; Tang, H.; Jia, B.; Wang, F.; Gan, Z. Polymer-doxorubicin conjugate micelles based on poly(ethyleneglycol) and poly(N-(2-hydroxypropyl) methacrylamide): effect of negative charge and molecular weight on biodistribution and blood clearance. *Biomacromol.* **2015**, *16*, 2645-2655.

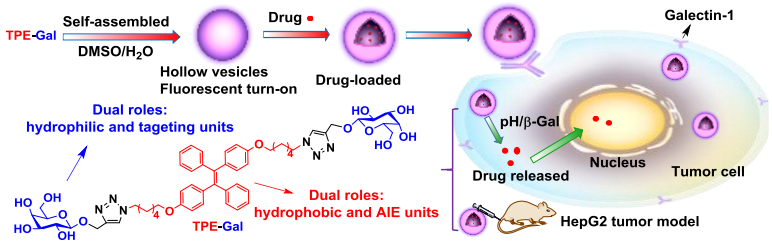

Insert Table of Contents artwork here